



INFLUENCE OF OXIDE FLUXES AND DUPLEX FLUXES ON MICROSTRUCTURAL, MECHANICAL PROPERTIES, AND WELD MORPHOLOGY OF A-TIG AH-36 STEEL WELDMENTS

¹K. Vijaya Kumar, ²N. Ramanaiyah, ³N. Bhargava Rama Mohan Rao³, K. Narendra Kumar⁴.

¹Assistant Professor, ²Professor, ³Professor, ⁴Assistant Professor

¹Dept.of Mechanical Engineering GIT, GITAM University, Visakhapatnam, India

²Dept.of Mechanical Engineering, Andhra University, Visakhapatnam, India

³Dept.of Metallurgical Engineering, Andhra University, Visakhapatnam, India

⁴Dept.of Mechanical Engineering GIT, GITAM University, Visakhapatnam, India

Abstract: In the field of Metallurgy, a flux is either chemical cleaning, a flowing or a purifying agent. They can be used either for extractive or metal joining. The current study aims to investigate the metallurgical, mechanical, and weld morphology of "AH36" marine grade steel with an 8mm thickness by "A-TIG" butt weld joints using a multitude of fluxes, such as TiO₂, Fe₂O₃, SiO₂, ZnO, MoO₃, and V₂O₅, as well as a duplex of TiO₂ 50% + Fe₂O₃ 50%, SiO₂ 50% + ZnO 50%, and MoO₃ 50% + V₂O₅ 50%. at the same process variables, with welding speed, held constant at 120mm/min and current 200Amp. In this study, have been carefully analyzed the depth (D), width (W), and depth/width (D/W) ratio of the weld bead, as well as the heat input behavior, were analyzed and as compared to traditional TIG (Tungsten Inert Gas) welding. In the due process it observed that the application of duplex flux produced a significant depth of penetration (more than base metal plate thickness) and less heat input. Further, we have investigated weld geometrical dimensions and uncovered the two primary reasons for improved weld bead dimensions were reverse Marangoni transformation and arc constriction. Furthermore, metallurgical characterization, mechanical properties of weldments generated by oxide fluxes were investigated using optical microscopy, SEM(EDS), Vickers micro-hardness, and tensile properties with MAKE-M/S Instron (Model no: 8801) in contrast to conventional TIG welding. The resulted microstructure, micro-hardness, and tensile profiles revealed that duplex fluxes coated welds had better mechanical properties than normal TIG.

Keywords: A-TIG Welding, AH36 steel, F.Z, HAZ, PM, weld bead depth, weld bead width

I. INTRODUCTION.

Aside from TIG welding, gas tungsten arc welding (GTAW) creates an arc between a non-consumable tungsten electrode and workpiece. In a protective gas environment, the workpieces are welded. Seng et al. [1] proposed the TIG welding technique. Due to its high weld quality and significant weld precession has become the most often used welding process. The TIG welding procedure is used to make aircraft components and components for the navy and defense academy K.H. Tseng and colleagues et al. [2,3]. The TIG welding procedure had one major flaw: it could only generate a limited number of thick and wide joints. Furthermore, the approximate thickness is to be welded up to 3mm; it necessitates edge preparation and multi-pass welding after 3mm; according to comparison studies, 3mm full depth can be achieved in TIG weldments on stainless steels with a single pass, according to comparison studies conducted by Sakthivel et al. [4]. A-TIG welding was proposed by Fujii et al. [5] to improve productivity, weld pool depth penetration, and weld form. Le Conte S et al. [6] observed that utilizing an inorganic powder termed activating flux, which is applied to metals before welding, might improve welding limits. When the activating flux Fe₂O₃ was used, Kamal et al. [7] reported an increase in weld depth and a decrease in weld bead width Tseng K et al. [8] carried out a test work plan using A-TIG conversion in conjunction with various welding types. Similarly, oxygen dissolution in weld metal resulted in deep weld penetration and affected weld microstructure Zou, Y et al. [9]. In this work, the net heat generated was calculated. The voltage impact, on the other hand, has not been quantified. A 6-second arc exposure results in increased energy density, greater arc temperature, and longer time for electromagnetic Lorentz force, all of which assist the molten metal sinking Tathgir, S et al.

[10]. In comparison to traditional GTA welding, SiO₂ and TiO₂ demonstrated the most obvious results in improving weld pool depth Priya Chauhan et al. [11]. TIG welding for deep penetration was assessed, and active flux was simplified. Welding was done on a SUS304 S.S. plate with a thickness of 10 mm. It was discovered that when the gas volume flow rate increased, the oxygen concentration decreased. The shielding gas flow rate and the nozzle cap oversaw it. The weld depth was raised by gradually increasing the amount of helium used as a shielding gas Yoshiaki Morisada et al. [12].

However, with ternary fluxes, statistical algorithms are used to create a formulation based on the percentages of flux components, with the objective of increasing weld depth and mechanical properties. A.B. Patel and colleagues [13]. Binary fluxes enable optimum percentages to be achieved, which can improve the appearance, form, and mechanical qualities of welds Duhan, R et.al [14]. Shallow penetration, limited dilution, and a low deposition rate in a single pass are the major limitations of using GTAW for thick plates. Tseng, K. H., et al. [15]. The depth of penetration can be improved by applying activated flux, and the creep rupture life can be improved by it, according to the literature review. Mechanical properties improved, and productivity increased Siddharaj Prajapati et al. [16]. Nagaraju, S et al. [17] found the capacity of the response surface method and genetic algorithm technique to anticipate the influence of changing factors on responses. However, with ternary fluxes, statistical programs are used to create a formulation based on the percentages of flux components, with the objective of increasing weld depth and mechanical properties. Among those who have contributed to this work are Paul B. G et al. [18]. The arc constriction phenomenon in A-TIG welding has been well documented and published by several authors Vidyarthi, R. S et al. [19]. When comparing the width of the bead on the plate, A-TIG welding creates narrower welds than traditional TIG welding. Only with A-TIG welding at 200 A and a speed of 7,8 cm/min was full penetration obtained M Jurica et al. [20]. ATIG welds have a greater tensile strength than TIG or parent metal welds (618MPa). This has something to do with the creation of delta ferrite, which has exceptionally high mechanical characteristics. Among those who have contributed to this work are Abdeljlil Hdhibi et al. [21].

The mechanical characteristics of the flux-produced weld were investigated. Salawu E Y et al. [22] developed a flux powder for welding DMR-249A Shipbuilding Steel. The most emphasis has been paid to the Activated-flux TIG welding technique, which utilizes welding flux to help decrease bead width and increase weld penetration. The use of activating flux with the welding process is a common technique to increase the industrial efficiency and penetrating ability of the TIG welding process. S A Afolalu et al. [23]. When compared to multi-pass GTAW of various steels, welding performed by the A-TIG welding technology may have good mechanical qualities Sharma, P et al. [24]. Because of the effect of heat created, oxygen-based flux governs dendritic arm spacing and length, which can be regulated by the oxygen level in the weld. Higher oxygen concentration with higher heat generation dominates bigger grain size, long dendrite length, and longer dendritic arm spacing in A-TIG welding with SiO₂ and CrO₃ flux, according to Surinder Tathgir et al. [25]. The arc constriction phenomenon in A-TIG welding has been well documented and published by several authors Kumar, H et al. [26]. Nineteen compositions were made from three oxides (TiO₂, MoO₃, and SiO₂) using the simplex lattice degree four design, with the best result being 55 % TiO₂ + 45 % MoO₃. In comparison to standard TIG weld beads, the enhanced formula's depth weld was doubled (7.24 mm) (3.64 mm) Kamel Touileb et al. [27]. Because of Marangoni convection and arc constriction mechanisms, the A-TIG welding approach achieved maximum penetration utilizing MoO₃ flux, which is 107 percent greater than a standard TIG welded sample. MgO, SiO₂, CaF₂, and MgCl₂*6H₂O, for example, demonstrated a significant increase in weld penetration et al. [28].

The overall scope of this study is to A-TIG weld AH-36 marine-grade steel and investigate relevant weld morphology as well as mechanical properties of A-TIG welded joints such as tensile strength, microhardness, and impact strength experimentally. Parametric research was carried out to determine the best heat input and welding speed for achieving maximum tensile strength, impact strength, and microhardness in weld joints. In addition, there is a comparison of TIG and A-TIG weldments with various fluxes such as TiO₂, Fe₂O₃, SiO₂, ZnO, MoO₃, and V₂O₅, as well as a duplex of TiO₂ 50% + Fe₂O₃ 50%, SiO₂ 50% + ZnO 50%, and MoO₃ 50% + V₂O₅ 50%.

II. MATERIAL AND METHODS

2.1 Material Composition.

TIG and A-TIG weldments were performed on AH-36 steel in the current study. The chemical constitution of the workpiece material has been investigated utilizing the dry spectroscopic strategy presented in Table 2.1

Table 2.1 Chemical constitution of AH36 steel material Chemical form (By % weight)

	C	Si	Mn	P	S	Cr	Ni	Mo
	0.206	0.262	0.794	0.00457	0.0119	0.0521	0.0102	0.00475
	Cu	Nb	V	W	Ca	la	Ti	Zr
	0.0264	<0.00100	0.00061	<0.00100	0.00169	<0.00100	<0.00100	<0.00150
Base	Co	Zn	B	Al	Sn	Pb	As	Bi
	<0.00150	0.00224	<0.00020	0.0103	0.00480	0.00474	0.0202	<0.0040
	Ce	Sb	Te	Fe				
	<0.00300	<0.00100	<0.00100	98.6				

2.2 Mechanical properties of the workpiece material

Table 2.2: The mechanical properties of the workpiece material tested using MAKE-M/S Instron (Model no: 8801).

Properties	Value
Yield Strength 0.2%	289.36 Mpa
UTS	453.63 Mpa
Young's Modulus	25.24 Gpa

2.3 Tungsten inert gas welding unit

TIG Welded joints AH36 steels with a thickness of 8mm. The butt type of joint was prepared by using the 350lx model TIG welding machine.

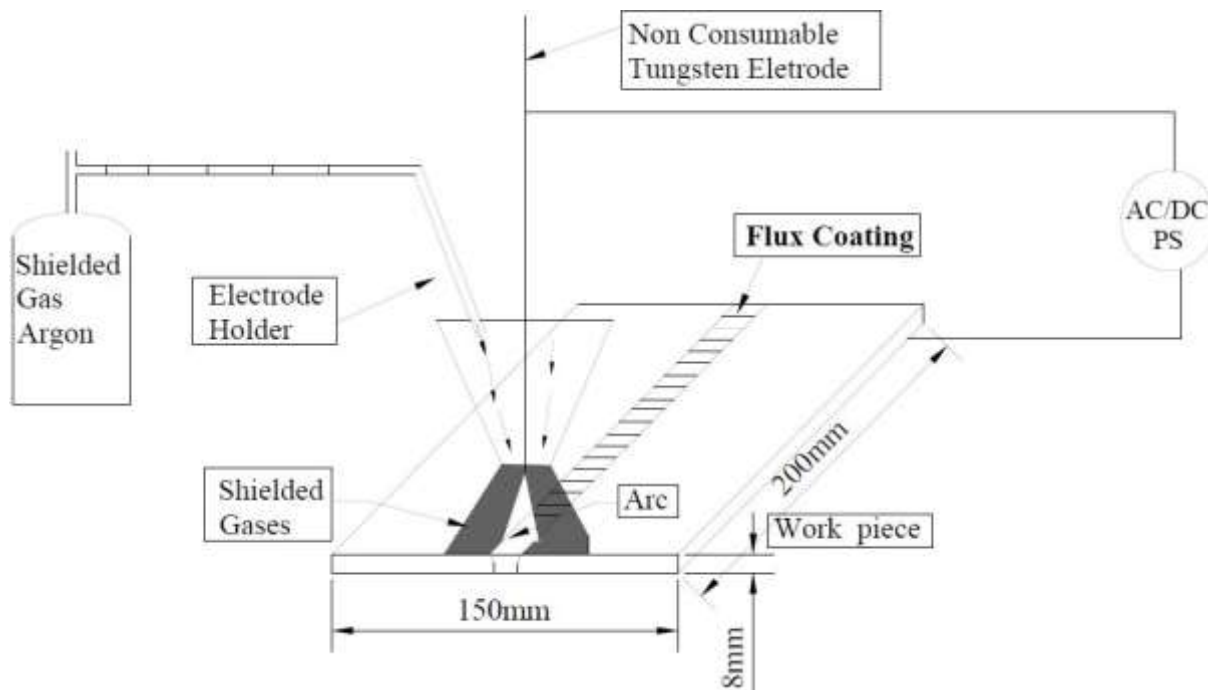


Figure 2.1: Schematic drawing of TIG Welding Unit

2.4 Experimental procedure

For the current investigation used hot rolled 8mm thick AH36 marine grade steel plates as a workpiece material. In this experiment by using the water wet machining (WJM) method, we cut the workpiece material into the desired shape and size, such as a rectangular shape with dimensions of 200mm×75mm×8mm as shown in Fig. 2.1 which depicts the butt-weld configuration. To remove the surface contaminants the 5mm sections of the work surfaces were polished with surface grinder and cleaned with acetone correlates with no gap between workpieces. Oxide fluxes such TiO₂, Fe₂O₃, SiO₂, ZnO, MoO₃, and V₂O₅, as well as a duplex of TiO₂ 50% + Fe₂O₃ 50%, SiO₂ 50% + ZnO 50%, and MoO₃ 50% + V₂O₅ 50% were weighted according to the volume applied and then mixed with acetone in a tiny cup using a stirrer. During the process, the workpieces were positioned in the butt position on the worktable indicated in Fig. 2.2. After the oxides-acetone mixer became like paste it was applied to the worktop surfaces of plates with 5mm width and 1mm thick on each side. According to Ahmadi and Ebrahimi [28], the activated flux thickness has a significant impact on penetration depth. Fitted in a nozzle is a tungsten thoriated electrode tip with a 30⁰-angle diameter and a 3mm diameter. Butt welding experiments were carried out utilizing 350lx automatic TIG welding equipment and direct current straight polarity (DCSP) power sources. During the procedure I observed the arc between the tungsten electrode and the workpiece was constant, and the inert gas protected it (argon). The welding current 200A and maintaining the welding speed at a steady 120mm/min consequently voltage varied automatically. By using the Water Jet Machining, the butt weldments were sliced into various types of sections to conduct different mechanical testing (WJM). A tensile test specimen was utilized according to ASTM E8/4M to utilize MAKE-M/S Instron (Model no: 8801) on weld joints with a limit of 100KN at a crosshead speed of 2 mm/min. During the procedure, on the components with dimensions of 50mm×15mm×8mm, the hardness estimations and large-scale/miniature structure examinations were performed. They cut the welding at a straight angle by keeping the weld zone in the middle. The samples were polished on a surface grinding machine and then mechanically ground polished with 1/0, 2/0, 3/0, and 4/0 grade papers, followed by a disc polishing machine using diamond paste as an abrasive medium to ensure a mirror-like image was obtained to reveal the microstructure of components that were etched in a 2% nital solution, followed by cleaning with deionized water and dipped in a solution of deionized water and dried with a drier an Inverted Optical microscope (Leica DMILM) used for microstructural characterization. Simultaneously, the composition of the fusion zone was examined using an energy-dispersive X-ray spectroscope (EDS) linked to a scanning electron microscope (SEM) with specifications of 6X to 600000X, detector SE, BSE, CCD. Furthermore, the I-Zod Impact Test Machine is used to determine the impact strength. The samples were produced and cut to I-Zod test specifications, such as 50mm×10mm×8 with a notch in the center. To measure microhardness

Shimadzu hardness equipment G20 was used in the indentation. The maximum capacity of this equipment was 2kg, and it gave hardness values directly by measuring the length of the diagonals. It had microscopes of 10X and 40X resolution so that it could measure the length of the diagonals. The Vickers hardness (HV) was calculated using:

$$VHN = 1.854 \frac{P}{d^2} \tag{1}$$

Here the load P was in 'gf,' and the mean diagonal d was in μm (this created hardness number units of $\text{gf}/\mu\text{m}^2$ despite the fact that the equivalent units kgf/mm^2 were chosen; in practice, the numbers are presenting place of the units). The Indentation tests can be performed on the specimen at different loads with different holding times. The holding times are used to test the dependency of the material on rate-dependent plasticity.

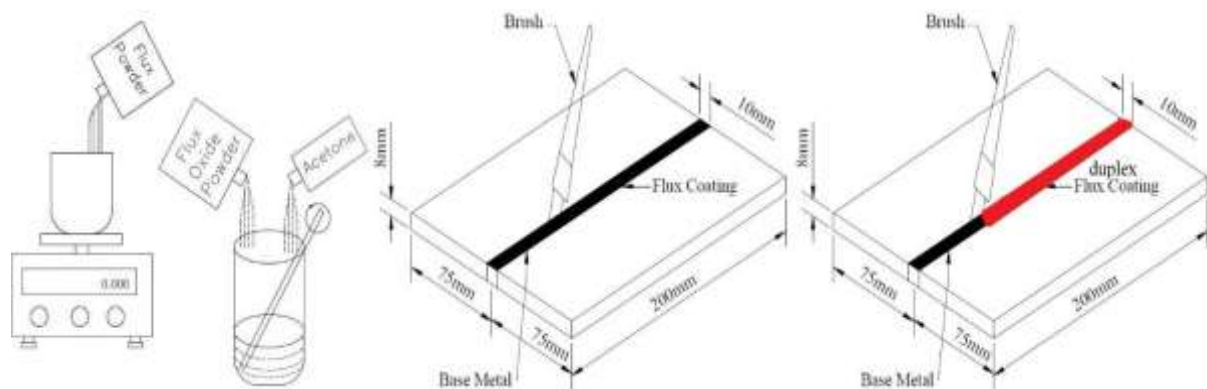


Figure 2.2: Illustration of complete A-TIG welding Process

III RESULTS AND DISCUSSIONS

3.1 Analysis of tensile behavior of weldments under various fluxes

The mean tensile strength and impact strength of TIG and A-TIG welding results are shown in Fig. 3.1 The tensile testing of the specimens has been conducted according to ASTM E8/4M to utilize MAKE-M/S Instron (Model no: 8801) on weld joints with a limit of 100KN at a crosshead speed of 2 mm/min. Parent fractures in all TIG and A-TIG weldments.

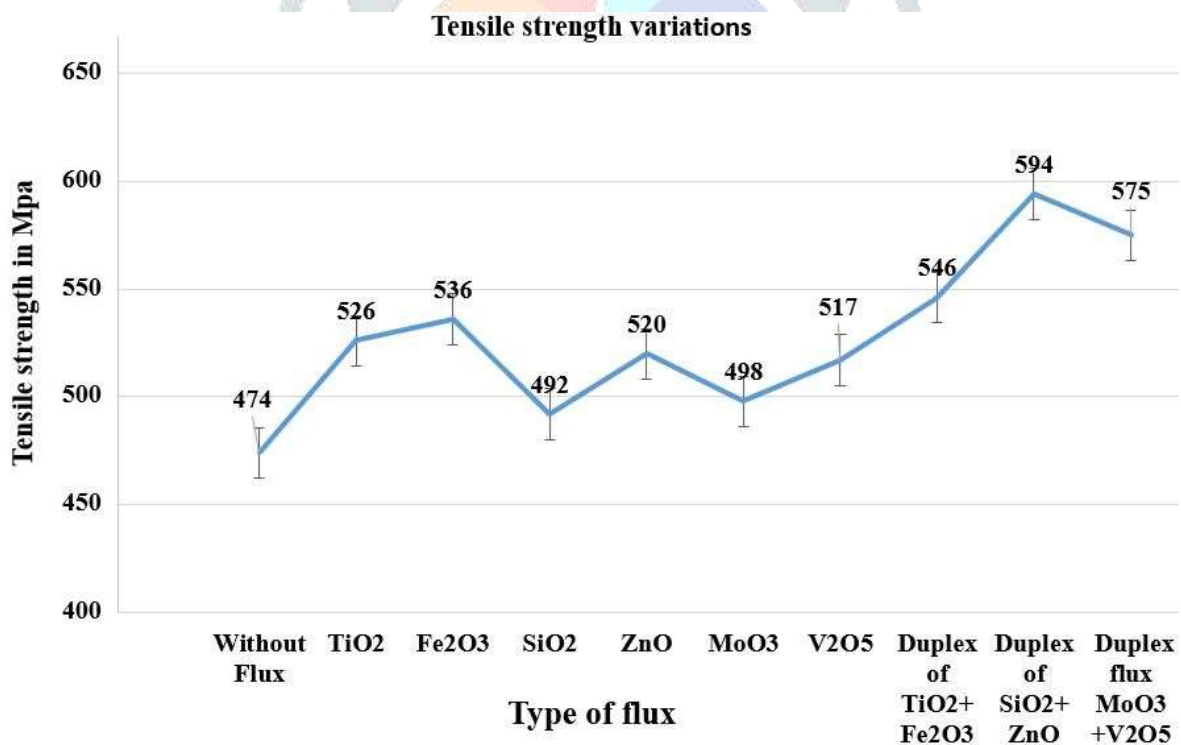


Figure 3.1: Tensile strength variations of various fluxes.

All flux-coated A-TIG weldments have significantly higher tensile and impact strength than ordinary TIG weldments. Furthermore, individual fluxes such as TiO₂, Fe₂O₃, SiO₂, ZnO, MoO₃, and V₂O₅ generate lower tensile strengths than duplex fluxes such as TiO₂ 50% + Fe₂O₃ 50%, SiO₂ 50% + ZnO 50%, and MoO₃ 50% + V₂O₅ 50% weldments. Besides the usage of individual fluxes, Fe₂O₃ flux coated weldment attains a high tensile strength of about 536 Mpa among all individual fluxes and base metal. When Fe₂O₃ flux coating is welded, free oxygen gives free electrons to the arc region, resulting in more heat being provided to the weld pool, faster melting, rapid cooling results in fine grain structure, and better will be tensile strength. However, all duplex results in higher tensile strengths rather the individual fluxes. Apart from that, the duplex of SiO₂ 50% + ZnO 50% flux coated weldments archives high tensile strength of about 594 Mpa. During welding with this flux, zinc reacts with oxygen to form

a layer that protects the weld pool from oxidation; no impurities can penetrate the weld pool, resulting in high tensile strength. On the other hand, Si acts as an alloying element in the weld region, leading to high tensile strength. Similar findings were reported by Vasanth raja et al. [29].

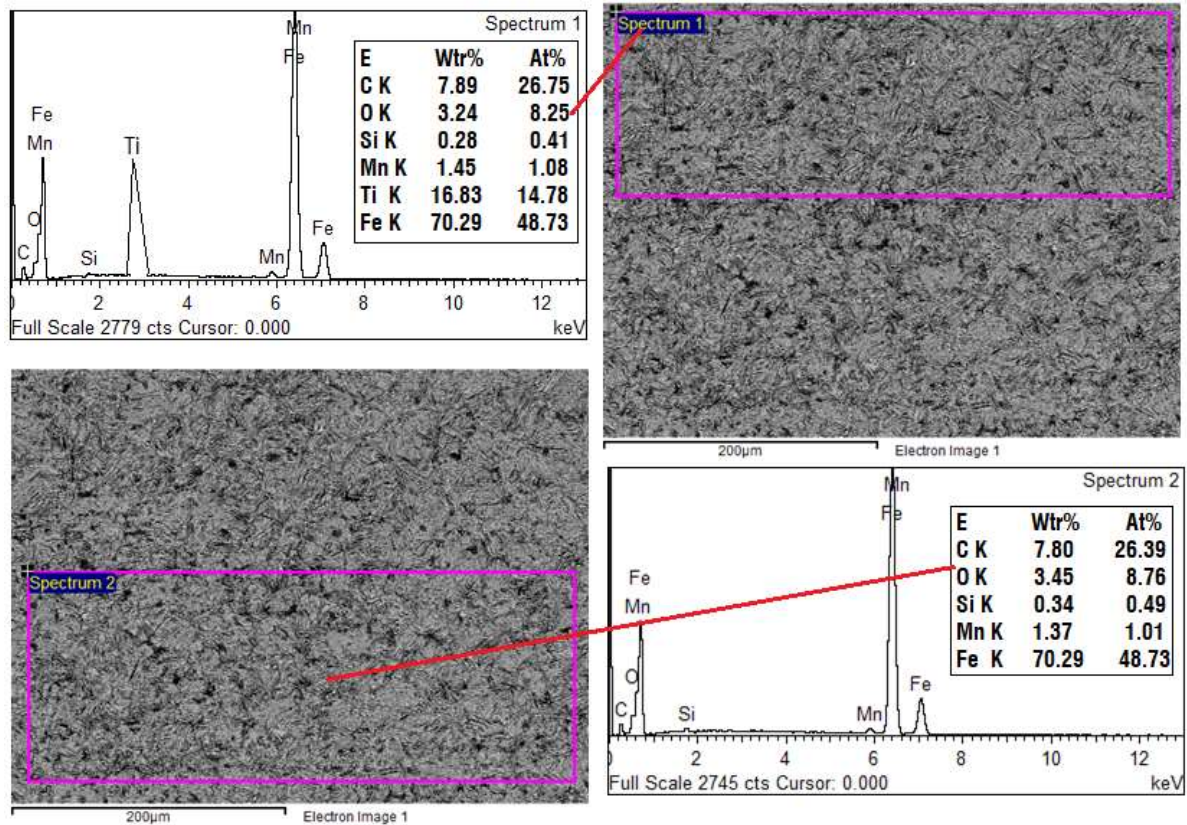


Figure 3.2: SEM result fusion zone TiO₂+Fe₂O₃ duplex coated weldments

The SEM-EDS findings in the weld area of A- TIG weldments of TiO₂ and Fe₂O₃ duplex Fig. 3.2 show that Ti is predicted to be about 15%, and Fe is expected to be approximately 70% of the alloying components. Ti elements give arc constriction because a stable arc is formed, which supplies a large amount of heat to the weld zone, and high Fe content leads to a high quantity of pearlite, which results in a high strength weld joint. Figure 3.3 shows that Mo and V are present in the weld area in proportions of 17% and 13%, respectively. These elements function as alloying elements in the weld area, resulting in excellent joint strength and ductility.

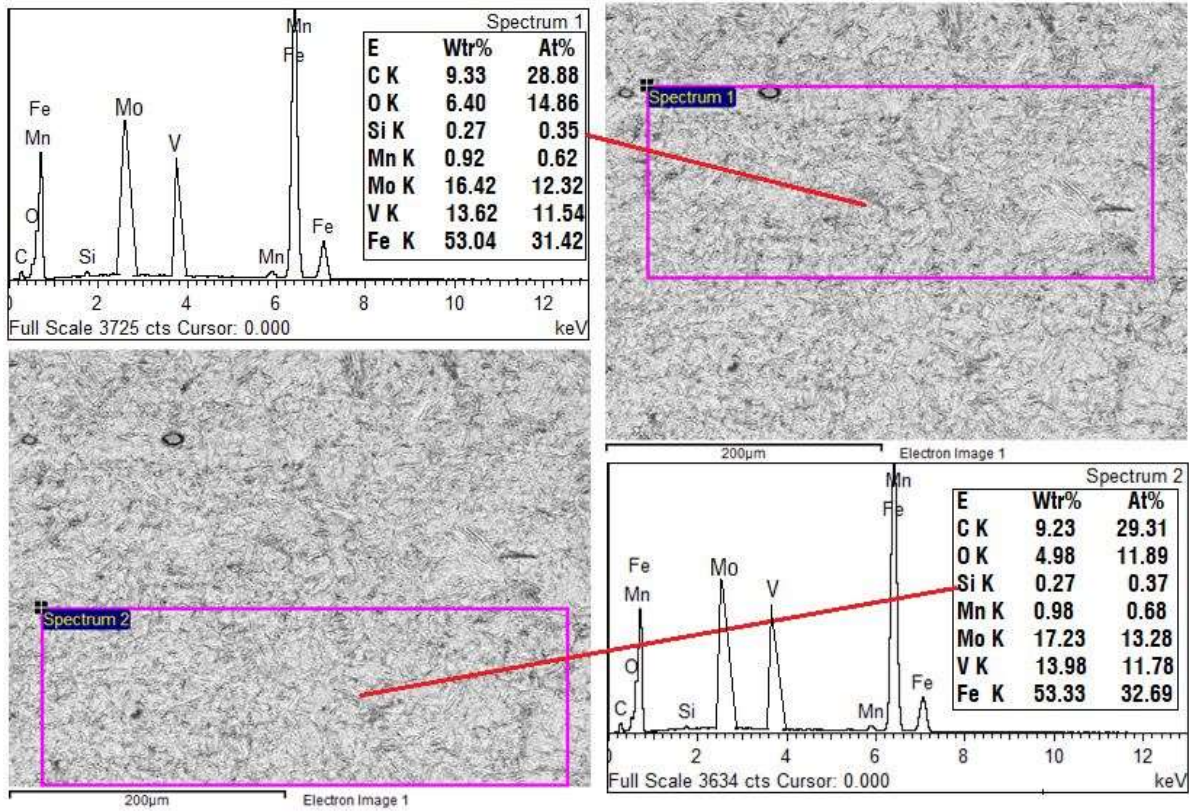


Figure 3.3: SEM result fusion zone of MoO₃+v₂O₅ duplex flux coating weldment

3.2 Analysis of impact behavior of weldments under various fluxes

Figure 3.4 depicts the impact behavior of different flux-produced weldments with process parameters of 200A current, welding speed 120 mm/min, and automated voltage.

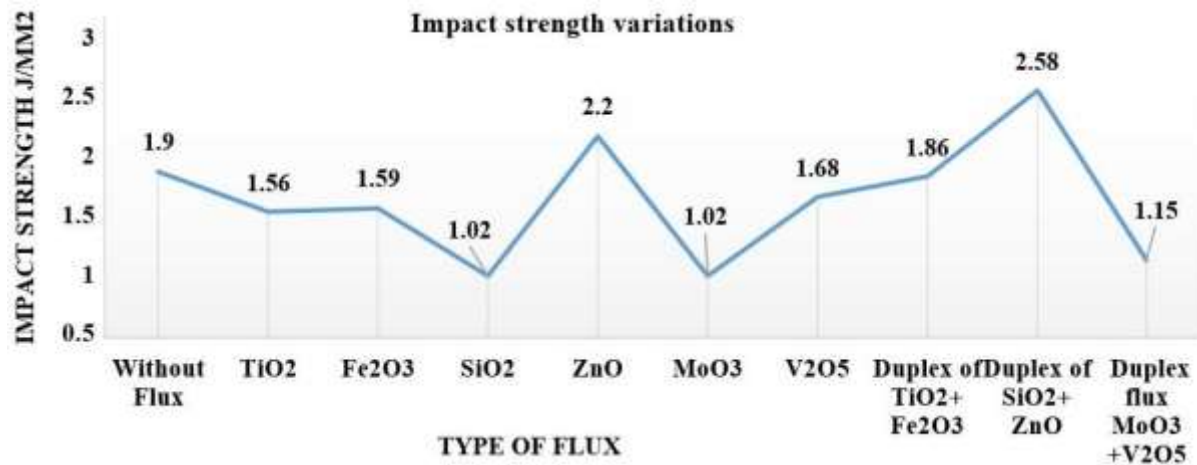


Figure 3.4: Impact strength variations of fluxes and duplex fluxes

Experiments show that ZnO and the duplex of ZnO+SiO₂ attempt great impact strength among all flux coated weldments. The ZnO flux coating weldment has 2.2 J/mm² and the duplex of ZnO+SiO₂ weldment has 2.5 J/mm² which is greater than the base metal and other flux coated A-TIG weldments. This is because Zn and Si serve as alloying elements in the fusion zone, enhancing impact strength, as described by Pratishtha Sharma et al. [30]. Figure 3.5 represents SEM-EDS data from the fusion zone of a 50 percent SiO₂ + 50 percent ZnO duplex flux coated weldment. The percentage of Zn and Si in the fusion zone is 12.5 % of Si and roughly 18% for Zn.

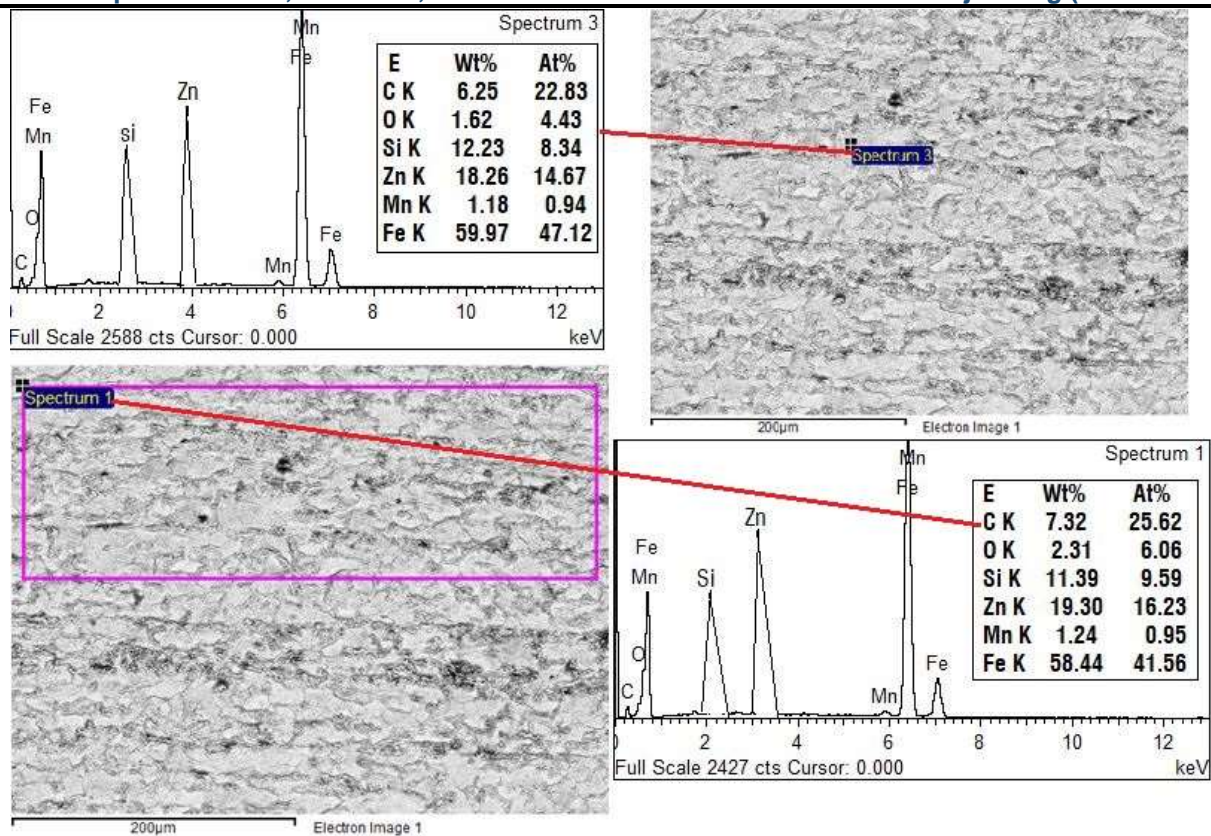


Figure 3.5: SEM result fusion zone of SiO₂+ZnO duplex flux coated weldment

3.3 Influence of oxide fluxes on weld bead dimensions

Oxide fluxes, a steady arc, and the reverse Marangoni effect were all brought into the weld pool. The use of fluxes modified the weld pool heat moment in TIG welding, resulting in diverse geometrical forms of weld beads. Surface tension decreases with increasing temperature, pure materials, and alloys in TIG welding. The surface tension of the weld pool mechanism was higher and is exceptionally low towards the margins compared to the middle of the weld pool, especially beneath the arc. As a result, molten metal flows from the joint center to the edges of the weld pool. Heat is transported from the center to the weld edges because of the mechanism, resulting in a broad width and reduced weld joint depth. This mechanism is known as the Marangoni transformation. Without flux coating, AH36 steel weldments with a low aspect ratio (D/W) of around 0.315, a more extended bead width (12.79mm), and little depth (4.04mm) of weld shapes were achieved in the current research result of Marangoni transformation. TIG welding using oxide fluxes such as TiO₂, Fe₂O₃, SiO₂, ZnO, MoO₃, and V₂O₅, as well as a duplex of TiO₂ 50% + Fe₂O₃ 50%, SiO₂ 50% +ZnO 50%, and MoO₃ 50% + V₂O₅ 50% commonly called A-TIG welding. These fluxes comprise surface-active elements such as oxide components, which are applied to the weld surface prior to welding, reversing the Marangoni transformation., the flow of molten metal from the edges to the center; this results in a considerable depth of weld joint and a smaller weld joint width.

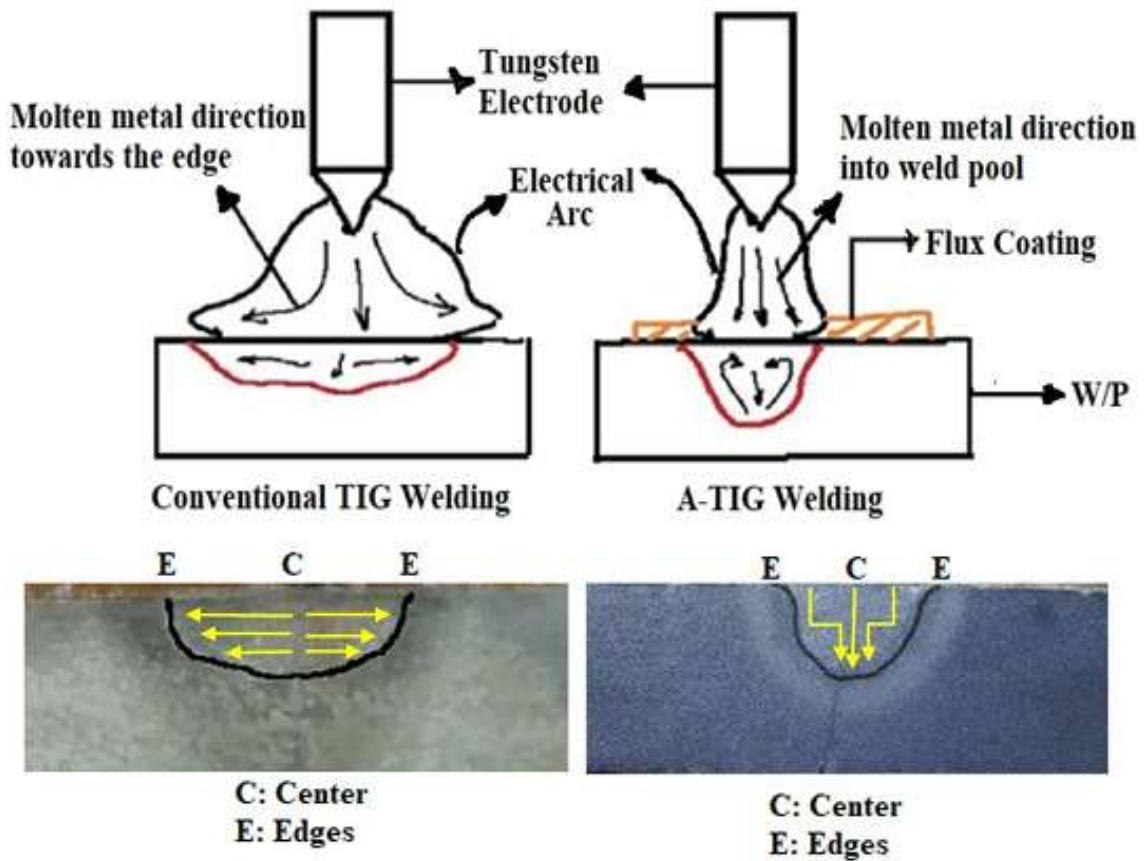


Figure 3.6: shows the distinctions between Marangoni and reverse Marangoni transformations

Figure 3.6 depicts the reverse Marangoni transformation as well as the difference between TIG and A-TIG welding. According to the experimental results, duplex coating weldments such as TiO_2 50% + Fe_2O_3 50%, SiO_2 50%+ ZnO 50%, and MoO_3 50 % + V_2O_5 50 % produced almost full penetration in the weld and less bead width when compared to individual flux coatings such as TiO_2 , Fe_2O_3 , SiO_2 , ZnO , MoO_3 , and V_2O_5 and conventional TIG weldments. Individual flux coating TiO_2 produces 7.12mm weld depth and 8.23mm width, while ZnO produces 6.91mm weld depth and 6.24mm width, both of which are better than standard TIG weldments. Figure 3.7 illustrates weld depth and width variations of various fluxes produced under the same process conditions.

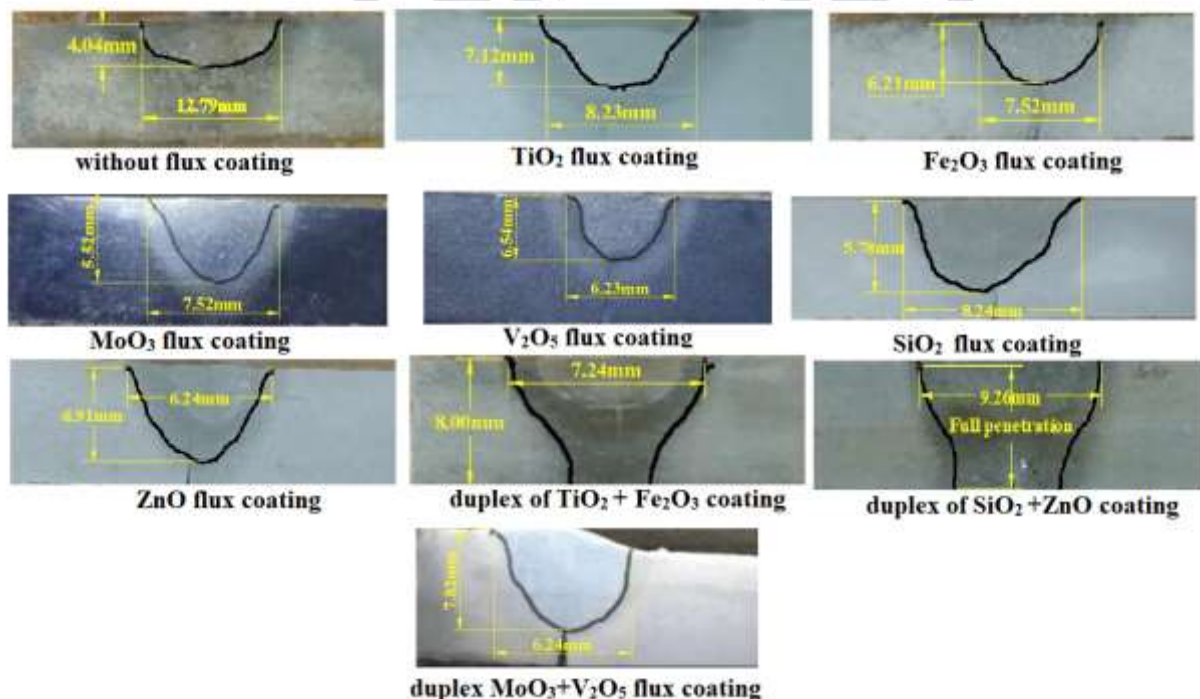


Figure 3.7 weld bead geometrical variations with the application of various fluxes

Apart from that, it is evident that the aspect varies somewhat with flux variation; nevertheless, it was discovered that TiO₂, ZnO, V₂O₅, and TiO₂ 50% + Fe₂O₃ 50%, SiO₂ 50% + ZnO 50%, and MoO₃ 50% + V₂O₅ 50% achieve high aspect ratios among all fluxes at the parameters. C.R. Heiple reported similar results [31], mainly in stainless steel weld joints. The depth, width, and aspect ratio variations without flux coated and various flux coated weldments are shown in Fig. 3.8. Lu S, Fujii H, and Nogi K [32] found that this resulted in a significant weld depth and a short weld bead width.

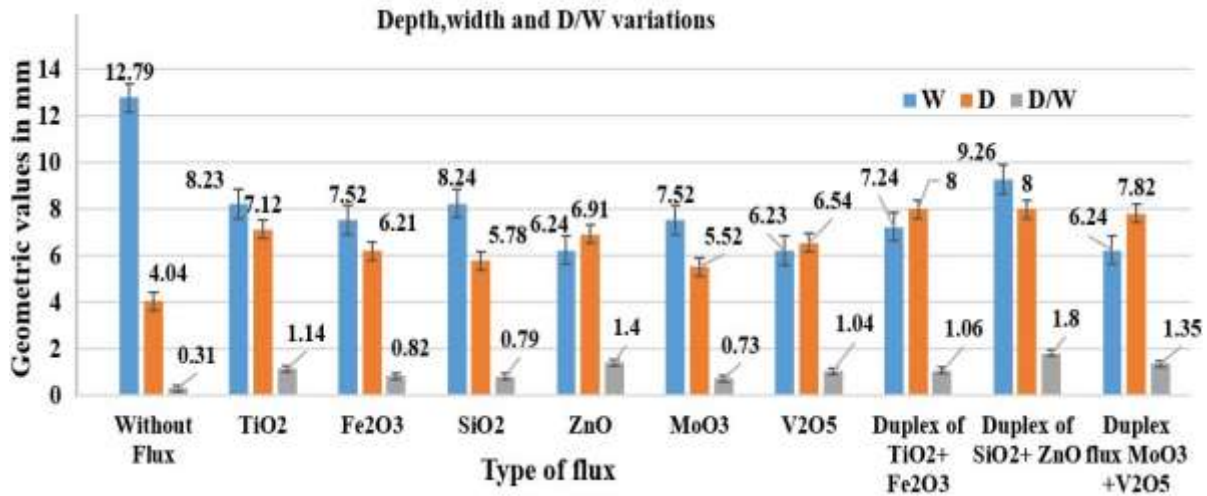


Figure 3.8 weld depth, width, and aspect variations of with different fluxes

3.4 The impact of oxide fluxes on Heat input

All TIG and A-TIG welding tests in this study employed direct current straight polarity.

To calculate heat input, use the formula below.

$$\text{Heat Input} = \frac{0.9 \times I \times V \times 60}{1000 \times S} \tag{2}$$

where V = arc voltage, I = arc current, S = welding speed and 0.9 = the arc efficiency (Arivazhagan and Vasudevan [33]).

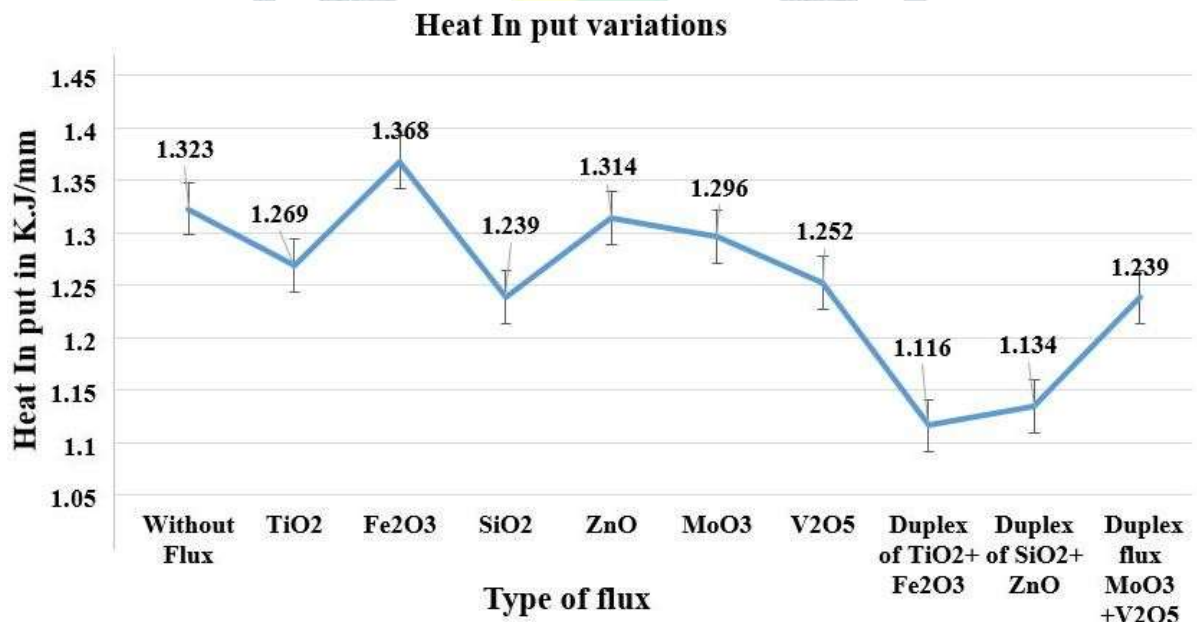


Figure 3.9 heat input variations of TIG and A-TIG weldments.

All TIG and A-TIG welding tests had their heat input estimated. It has been observed that the measured arc voltage was decrease with a constant current and welding speed calculated heat input depends on measured arc voltage in conventional TIG welding as well as A-TIG welding processes with shown in Fig. 3.9. The results show that without flux coating, Fe₂O₃ and ZnO flux coated weldments use more heat than other fluxes at the same parameters. This because without flux there will be a no free electron to supply arc region. However, in the case of Fe₂O₃, even though free electrons were accessible due to an abundance of

oxygen, they were not supplied to the arc area. In contrast, with flux coating, excessive oxygen reacts with zin to create a zinc layer, which acts as a shield for the weld pool. According to Hilkes J, Gross V [34], TIG welding with flux application significantly increases heat input magnitude during welding. Furthermore, more duplex fluxes have a higher weld depth with less heat input. This is because flux density impacts weld bead depth. According to Leconte S and Paillard P [6,] oxides can increase the energy flux density given to the metal by the arc. The amount of molten metal has always been proportionated to the amount of available heat energy.

3.5 Micro-hardness variations in weld regions under the application of fluxes

Micro hardness is determined in all three zones FZ, HAZ, and PZ of TIG and A-TIG weldments. It is noticed that the FZ of all A-TIG weldments dominates with greater hardness values when compared to the fusion zone of TIG and A-TIG weldments and showed in Fig. 3.10. The hardness HAZ of A-TIG weldments higher than the parent zone of weldments. The A-TIG welding with Fe₂O₃ flux have higher hardness 294VHN in FZ.

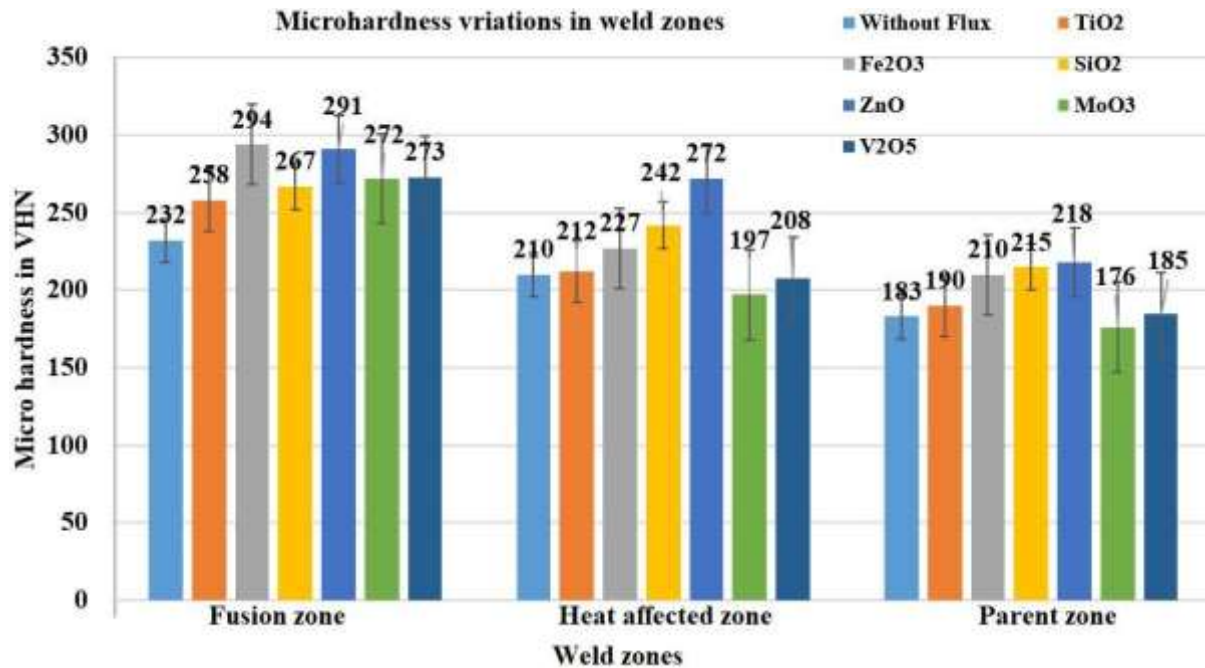


Figure 3.10 variations in micro hardness in the FZ, HAZ, and PZ of TIG and A-TIG weldments.

Because of the excessive Fe with the application of Fe₂O₃ coating, a greater quantity of pearlite dominates in the fusion zone, and as a result, increased hardness prevails in the fusion zone. In addition, ZnO flux coated weldments have greater micro hardness in all zones than all other weldments. This is because fluxes also act as alloying elements in the fusion zone, resulting in greater hardness dominating in the fusion zone. All Fusion Zone Micro Hardness values with and without flux coating weldments are higher than the heat-affected zone and parent Zone. Figure 3.11 compares microhardness values of conventional TIG and duplex flux coated weldments and clearly indicates that duplex flux coated weldments are superior in FZ, HAZ and PZ.

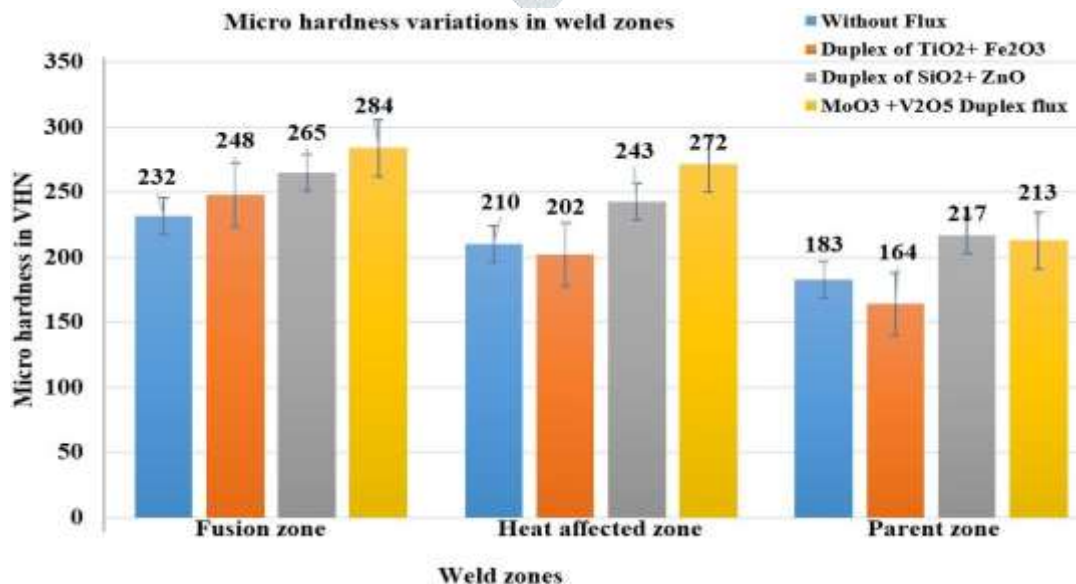


Figure 3.11 variations in micro hardness in the FZ, HAZ, and PZ of duplex flux coated A-TIG weldments

The reason behind this, From the Fig. 3.12 it is that the fusion zone has an equiaxed grain structure; as a result, it achieved the highest microhardness values among all three zones. On the other hand, the parent region has a coarse grain structure because it possesses less hardness. It also observed that HAZ has a fine grain structure; this leads to microhardness values fluctuated between PZ and FZ values. Similar reported by K. Devendra Nath Ramkumar et al. [35].

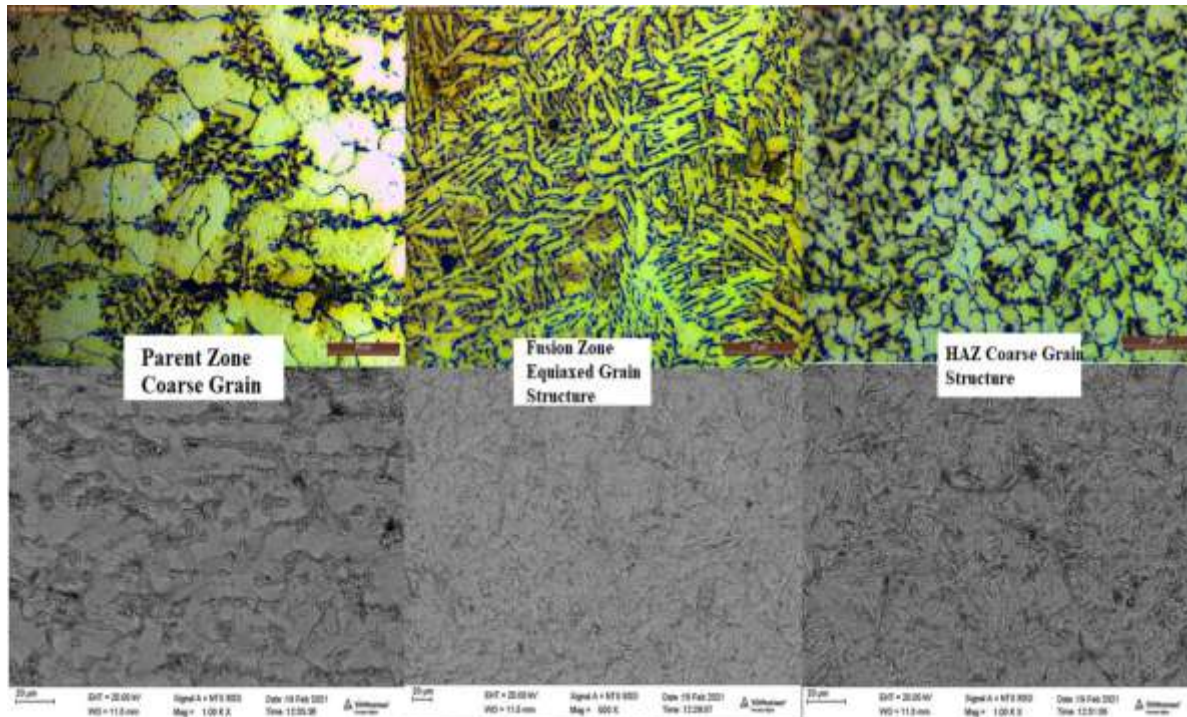


Figure 3.12 microstructure variation in PZ, FZ and HAZ in the weld portion

IV. CONCLUSION

The current study experiments led and examined TIG welding using oxide flux before the welding of two AH36 steel plates in butt position. The fluxes are utilized as follows TiO_2 , Fe_2O_3 , SiO_2 , ZnO , MoO_3 , and V_2O_5 , as well as a duplex of TiO_2 50% + Fe_2O_3 50%, SiO_2 50% + ZnO 50%, and MoO_3 50% + V_2O_5 50%. The principal results got and summed up as follows:

- (1). Inadequate high caliber and better appearance of the surface acquired of AH36 steel weldments with Activated flux and duplex flux TIG welding process.
- (2). The Mechanical properties of A-TIG welded AH36 weldments predominant than the ordinary TIG welding process.
- (3). Considering all fluxes experimental trails, duplex flux effectively used to weld AH36 steel 8mm thick plates in Butt position at 200Amp current and 120mm/min process parameters.
- (4) The tensile test behavior of duplex flux coated weldments attains higher than the individual flux coated and conventional TIG weldments.
- (5). Higher weld depth of penetration accomplished of the weld joint with the use of duplex flux (8mm), TiO_2 (7.12mm), ZnO (6.91mm), MoO_3 50% + V_2O_5 50% (7.82mm) and TiO_2 50% + Fe_2O_3 50%, SiO_2 50% + ZnO 50% produce full penetration, and these higher than the conventional TIG weldments at current 200A, welding speed 120mm/min and measured arc voltage parameters.
- (6). The purpose behind the higher depth of penetration was the impact of Marangoni transformation, stable arc, and arc constriction choking resulting from oxide fluxes.
- (7). The heat input results noticed that there was a significant increase due to the usage of oxide fluxes. Up to this time, the activated flux coating TIG welding process could enhance the electric arc voltage. The magnitude of heat input per unit length in a weld is also greatly enlarged. Hence, the delta-ferrite amount in the weld region material could be enhanced. However, in addition to that, usage of oxide flux coating on work surfaces before welding does not significantly impact the hardness of welded joints.
- (8). The A-TIG welding method can Increase the welds aspect ratio and is made sure the greatest of duplex of TiO_2 + Fe_2O_3 flux (1.06), MoO_3 + V_2O_5 flux (1.35), SiO_2 + ZnO (1.80) and ZnO (1.4) compare with the traditional TIG welding method.
- (9) In this study, the microstructure considers showing that columnar structure and equiaxed in the fusion zone using oxide fluxes, which drives predominant mechanical properties than the ordinary TIG welding.

V. Acknowledgments

Acknowledgments Author is grateful to the Indian Institute of Technology Madras, India, for providing an opportunity for conducting experimental work required for the investigation. Hindustan Shipyard Pvt Ltd (HSL), Visakhapatnam, India, for sponsoring the raw material for research works, and GITAM University Visakhapatnam, India for their support for conducting experimental work analysis.

REFERENCES

- [1] Tseng, KH. Hsu, CY. 2011. Performance of activated TIG process in austenitic stainless-steel welds. *Journal of Materials Processing Technology*, 211(3): 503–512.
- [2] Tseng, K.H. Chuang, K.J. 2012. Application of iron-based powders in tungsten inert gas welding for 17Cr–10Ni–2Mo alloys. *Powder Technology*, 228:36–46.
- [3] Tseng, K.H. Chen, K.L. 2012. Comparisons between TiO₂- and SiO₂-flux assisted TIG welding processes, *Journal of Nanoscience and Nanotechnology* 12 (2012) 6359–6367.
- [4] Sakthivel, T. Vasudevan, M. Laha, K. Parameswaran, P. Chandravathi, KS, Mathew, MD. 2011. Comparison of creep rupture behaviour of type 316L(N) austenitic stainless-steel joints welded by TIG and activated TIG welding processes. *Materials Science Engineering*, 528(22–23):6971–80.
- [5] Fujii, H. Sato, T. Lu, S. Nogi, K. 2008. Development of an advanced A-TIG (AA-TIG) welding method by control of Marangoni convection. *Materials Science Engineering*, 495:296–303.
- [6] Leconte, S. Paillard, P. Chapelle, P. Henrion, G. Saindrenan, J. 2006. Effect of oxide fluxes on the tungsten inert gas process's activation mechanisms. *Science and Technology of Welding and Joining*, 11(4):389–97.
- [7] Kamal, H. Dhandha, Vishvesh, J. Badheka. 2015. Effect of activating fluxes on weld bead morphology of P91 steel bead-on-plate welds by flux assisted tungsten inert gas welding process. *Journal of Manufacturing Processes*, 17: 48–57.
- [8] Tseng, K. 2013. Development and application of oxide-based flux powder for tungsten inert gas welding of austenitic stainless steels. *Powder Technology*, 233: 72–79.
- [9] Zou, Y. Ueji, R. Fujii, H. 2014. Effect of Oxygen on Weld Shape and Crystallographic Orientation of Duplex Stainless-Steel Weld Using Advanced A-TIG (AA-TIG) Welding Method. *Material Characteristics*, 91: 42–49.
- [10] Tathgir, S. Bhattacharya, A. Bera, T. K. 2015. Influence of Current and Shielding Gas in TiO₂ Flux Activated Tig Welding on Different Graded Steels. *Materials and Manufacturing Processes*, 30(9): 1115–1123.
- [11] Priya, Chauhan. Hemant, Panchal. 2016. A Review on Activated Gas Tungsten Arc Welding (A-GTAW). *IJSDR*, Vol 1, Issue 5.
- [12] Yoshiaki, Morisada. Hidetoshi, Fujii. Ni, Xukun. 2014. Development of simplified active flux tungsten inert gas welding for deep penetration. *Materials and Design*, 54: 526–530.
- [13] Patel, A.B. Patel, S.P. 2014, The effect of activating fluxes in TIG welding by using Anova for SS 321. *Int. J. Eng. Res. Appl*, 4: 41–48.
- [14] Duhane, R. Choudhary, S. 2015. Effect of Activated Flux on Properties of SS 304 Using TIG Welding. *Int. J. Eng. Trans. B*, 28: 290–295.
- [15] Tseng, K.H. Chen, P.Y. 2016. Effect of TiO₂ Crystalline Phase on Performance of flux Assisted GTA Welds. *Materials and Manufacturing Process*, 31(3),359–365.
- [16] Siddha raj, Prajapati. Ketan, Shah. 2016. Experimental Study on Activated Tungsten Inert Gas Welding- A Review paper *IJARIE*, 2(3):2395-4396.
- [17] Nagaraj, S. Vasanth raja, P. Chandrasekhar, N. Vasudevan, M. Jayakumar, T. 2016. Optimization of Welding Process Parameters for 9cr-1mo Steel Using RSM and GA. *Material and Manufacturing Process*, 31(3):319–327.
- [18] Paul, B.G. Ramesh Kumar, K.C. 2017. Effect of single component and binary fluxes on the depth of penetration in a-TIG welding of Inconel alloy 800H austenitic stainless steel. *International Journal of Advanced Engineering and Global Technology*, 5, 1791–1795.
- [19] Vidyarthi, R. S. Dwivedi, D. K. Muthu Kumaran, V. 2018. Optimization of A-TIG Process Parameters Using Response Surface Methodology. *Materials and Manufacturing Processes*, 33(7):709-717
- [20] Jurica, M. Kozuh, Z. 2018. Optimization of the A-TIG welding for stainless steels. *IOP Conference Series. Materials Science & Engineering*. 329: 012012.
- [21] Hdhibi, A. Touileb, K. Djoudjou, R. Ouis, A. Bouazizi, ML. Chakhari, J. 2018. Effect of Single Oxide Fluxes on Morphology and Mechanical Properties of ATIG on 316 L Austenitic Stainless-Steel Welds. *Engineering, Technology & Applied Science Research*, 8(3): 3064-3072
- [22] Salawu, E .Y. Okokpujie, I. P. Afolalu, SA. Ajayi, O. Azeta, J. 2018. Investigation of production output for improvement. *International Journal of Mechanical and Production Engineering Research and Development*, 8(1) 915-922.
- [23] Afolalu, SA. Soetan, SB. Ongbali, SO. Abioye, AA. Oni, AS. 2019. Impact of activated–flux tungsten inert gas (a-tig) welding on weld joint of a metal. *Materials Science and Engineering*, 640(1):012064.
- [24] Sharma, P. Dwivedi, D. K. 2019. Comparative Study of Activated Flux-GTAW and Multipass-GTAW Dissimilar P92 Steel-304H ASS Joints. *Materials and Manufacturing Processes*. 34(11): 1195-1204
- [25] Surinder, Tathgir. Dinesh, W. Rathod & Ajay, Batish. 2019. A-TIG welding process for enhanced-penetration in Duplex stainless-steel: effect of activated fluxes? *Materials and Manufacturing Processes*: 1042-6914.
- [26] Kumar, H. Ahmad, G. N. Singh, N. K. 2019. Activated Flux TIG Welding of Inconel 718 Super Alloy in Presence of Tri-Component Flux. *Mater. Manuf. Process*, 34(2): 216–223.
- [27] Touileb, K. Ouis, A. Djoudjou, R. Hedhibi, AC. Alrobei, H. Albaijan, I. 2020. Effects of A-TIG welding on weld shape, mechanical properties, and corrosion resistance of 430 ferritic stainless steel alloy. *Metals (Basel)*, 10(3).
- [28] Rana, H. Badheka, V. Patel, P. Patel, V. Li, W. Andersson, J. 2021. Augmentation of weld penetration by flux assisted TIG welding and its distinct variants for oxygen free copper. *Journal of Materials Processing Technology*, 10:138–151.
- [29] Vasantharaja, P. Vasudevan, M. 2012. Studies on A-TIG welding of low activation ferritic/martensitic (LAFM) steel. *Journal of Nuclear Materials*, 421: 117–123.
- [30] Prathishtha, Sharma. Dheerendra Kumar, Dwivedi. 2021. Improving the strength-ductility synergy and impact toughness of dissimilar martensitic-austenitic steel joints by A-TIG welding with wire feed. *Materials letters*, 285: 129063.
- [31] Heiple, CR. and Roper, JR. 1982. *ASM Conf. Trends in Welding Research in the United States*, New Orleans, LA :489–515.
- [32] Lu, S. Fujii, H. Nogi, K. 2004. Marangoni convection and weld shape variations in Ar–O₂ and Ar–CO₂ shielded GTA welding. *Materials Science Engineering*, 380:290–297

- [33] Arivazhagan, B. Vasudevan, M. 2013. A study of microstructure and mechanical properties of grade 91 steel A-TIG weld joint. *Journal of Materials Engineering and Performance*, 22(12):3708–3716.
- [34] Hilkes, J. Gross, V. 2013. Welding Cr-Mo steels for power generation and petrochemical applications. past, present, and future. *Biul Instyt Spawalnictwa*, 2:11–22.
- [35] Devendranath Ramkumar, Jelli. Lakshmi Narasimha, Varma. Gangineni, Chaitanya. Ayush, Choudhary. N, Arivazhagan, S, Narayanan. 2015. Effect of autogenous GTA welding with and without flux addition on the microstructure and mechanical properties of AISI904L joints *Materials Science & Engineering A*, 636: 1–9.

